Metrology with PT-Symmetric Cavities: Enhanced Sensitivity near the PT-Phase Transition

Zhong-Peng Liu, Jing Zhang, Şahin Kaya Özdemir, Bo Peng, Hui Jing, Xin-You Lü, Chun-Wen Li, Lan Yang, Franco Nori, and Yu-xi Liu

Phys. Rev. Lett. **117**, 110802 — Published 7 September 2016

DOI: 10.1103/PhysRevLett.117.110802

Metrology with $\mathcal{PT}$-symmetric cavities: Enhanced sensitivity near the $\mathcal{PT}$-phase transition

Zhong-Peng Liu,[1,2] Jing Zhang,[1,2,3,4,*] Şahin Kaya Özdemir,[3,†] Bo Peng,[3] Hui Jing,[4,5] Xin-You Lü,[4,6] Chun-Wen Li,[1,2] Lan Yang,[3] Franco Nori,[4,7] and Yu-xi Liu[2,8]

[1]*Department of Automation, Tsinghua University, Beijing 100084, P. R. China*
[2]*Tsinghua National Laboratory for Information Science and Technology, Beijing 100084, P. R. China*
[3]*Department of Electrical and Systems Engineering, Washington University, St. Louis, MO 63130, USA*
[4]*CEMS, RIKEN, Saitama 351-0198, Japan*
[5]*Key Laboratory of Low-Dimensional Quantum Structures and Quantum Control of Ministry of Education, Department of Physics and Synergetic Innovation Center for Quantum Effects and Applications, Hunan Normal University, Changsha 410081, China*
[6]*School of physics, Huazhong University of Science and Technology, Wuhan 430074, P. R. China*
[7]*Physics Department, The University of Michigan, Ann Arbor, MI*
[8]*Institute of Microelectronics, Tsinghua University, Beijing 100084, P. R. China*

(Dated: August 10, 2016)

We propose and analyze a new approach based on parity-time ($\mathcal{PT}$) symmetric microcavities with balanced gain and loss to enhance the performance of cavity-assisted metrology. We identify the conditions under which $\mathcal{PT}$-symmetric microcavities allow to improve sensitivity beyond what is achievable in loss-only systems. We discuss the application of $\mathcal{PT}$-symmetric microcavities to the detection of mechanical motion, and show that the sensitivity is significantly enhanced near the transition point from unbroken- to broken-$\mathcal{PT}$ regimes. Our results open a new direction for $\mathcal{PT}$-symmetric physical systems and it may find use in ultra-high precision metrology and sensing.

PACS numbers: 42.65.Yj, 06.30.Ft, 42.50.Wk

Introduction.— The measurement of physical quantities with high precision is the subject of metrology. This has attracted much attention due to increasing interest in, e.g., gravitational wave detection [1], sensing of nanostructures [2, 3], global positioning and navigation [4, 5]. Developments in metrology over the past two decades have provided necessary tools to determine the fundamental limits of measuring physical quantities and the resources required to achieve them [6, 7]. Techniques that will help to reach the fundamental detection limit and measure very weak signals are being actively sought.

Among many different approaches, cavity-assisted metrology (CAM), where a cavity or a resonator with high-quality (Q) factor is coupled to a device under test (DUT), has emerged as a versatile and efficient approach for high-precision measurements. The coupling between the resonator and the DUT manifests itself as a back-action-induced frequency shift, mode splitting, or a sideband in the output transmission spectrum [8]. CAM has been applied for reading out the state of a qubit [9], measuring tiny mechanical motions [10–16] and detecting nanoparticles [17, 18].

The readout signal (i.e., the transmission spectrum) of CAM is determined by the sum of the background spectrum of the cavity and the back-action spectrum of the DUT. The background spectrum is determined by the Q of the cavity, whereas the back-action spectrum is determined by the strength of the cavity-DUT coupling (also dependent on Q) and the quantity to be measured. A broad background spectrum masks the back-action spectrum and decreases the signal-to-noise ratio (SNR) [Fig. 1(a)]. A higher cavity-DUT coupling strength and a higher Q help to detect very weak signals, and enable to resolve fine structures in the output spectra [Fig. 1(b)]. CAM will benefit significantly from a narrower background spectrum which is limited by the cavity losses.

In this Letter, we show that the performance of CAM is significantly enhanced if the passive cavity (i.e., lossy; without optical gain) of the CAM is coupled to an auxiliary cavity with optical gain (i.e., active cavity) that balances the loss of the passive cavity. Such coupled structures with balanced gain and loss form parity-time ($\mathcal{PT}$) symmetric systems [19], which have been widely studied theoretically [20–29] and experimentally [30–38].

As a specific application of $\mathcal{PT}$-CAM, we show the enhancement in the detection of the motion of a nanomechanical resonator placed in the proximity of the passive microcavity of $\mathcal{PT}$-CAM. The enhancement is significant near the $\mathcal{PT}$-phase transition point through which the system transits from broken- to unbroken-$\mathcal{PT}$ symmetry. The mechanism for the enhancement of the measurement sensitivity in our system is attributed to two features. First, due to gain-loss balance the supermodes are almost lossless (extremely high-Q), and the background spectrum is much narrower. Thus, it is easier to resolve the sideband induced by the DUT. Second, the effective interaction strength between the optical modes and the DUT is significantly enhanced. Therefore, even very weak perturbations lead to significant changes in the

spectrum and hence become detectable.

Cavity-assisted metrology (CAM) with $\mathcal{PT}$-symmetric microcavities.— The traditional CAM is composed of a lossy optical cavity coupled to a DUT [Fig. 1(a)]. The interaction Hamiltonian is given by $H_{\rm int} = ga^\dagger az$, where a is the cavity's annihilation operator; z is the DUT's observable being measured; and g is the strength of the DUT-cavity coupling. In order to realize the $\mathcal{PT}$-CAM, an active cavity is directly coupled to a lossy cavity [Fig. 1(b)], similar to the configuration discussed in Ref. [38], and the DUT is directly coupled to the lossy cavity. Here the inter-cavity coupling strength is controlled by the distance between the cavities, and the gain-to-loss ratio of the cavities is adjusted by an electrical or optical pump exciting the optical-gain providing material of the active cavity. The Hamiltonian describing this $\mathcal{PT}$-CAM system is given by

$$H = (\Delta - i\kappa)\, a^\dagger a + (\Delta + i\gamma)\, c^\dagger c + ga^\dagger az + g_1(a^\dagger c + c^\dagger a), \tag{1}$$

where c is the annihilation operator of the active cavity; κ and γ, respectively, denote the loss and gain rates of the passive and active cavities; g_1 is the inter-cavity coupling strength; and Δ corresponds to the effective frequencies of the cavities.

Without the interaction term $ga^\dagger az$, Eq.(1) accounts for the coupling between the optical modes of the microcavities, and leads to two supermodes $a_\pm$ that are described with the complex eigenfrequencies $\omega_\pm = \Omega_\pm - i\Gamma_\pm = \Delta - i\chi \pm \beta$, where $\beta = \sqrt{g_1^2 - \Gamma^2}$, $\chi = (\kappa - \gamma)/2$, $\Gamma = (\gamma + \kappa)/2$; $\Omega_\pm$ and $\Gamma_\pm$ denote, respectively, the frequencies and the decay rates of the supermodes. Clearly, β experiences a transition from a real to an imaginary value and vice versa at $\Gamma = g_1$, where $\beta = 0$. At the transition point, the eigenfrequencies coalesce, that is $\omega_\pm = \Delta - i\chi$.

For $\Gamma < g_1$, β is real (denoted as $\beta = \beta_r$), and the complex eigenfrequencies become $\omega_\pm = \Delta \pm \beta_r - i\chi$, implying that two supermodes have different resonance frequencies $[\Omega_- \neq \Omega_+]$, but the same damping rates and linewidths $[\Gamma_\pm = \chi]$. The separation of resonance frequencies (i.e., amount of mode splitting) is given by $2\beta_r$. For $\Gamma > g_1$, on the other hand, β is imaginary, $(\beta = i\beta_r)$, and the complex eigenfrequencies become $\omega_\pm = \Delta - i(\chi \mp \beta_r)$, implying two frequency-degenerate supermodes $[\Omega_\pm = \Delta]$ with different damping rates and linewidths $[\Gamma_\pm = \chi \mp \beta_r]$.

When the gain γ of the active cavity balances the loss κ of the passive cavity, $\beta = 0$ corresponds to a *$\mathcal{PT}$-phase transition point*, where the supermodes coalesce, and χ becomes zero, implying lossless supermodes. The regime defined by $\Gamma < g_1$ corresponds to the *$\mathcal{PT}$-symmetric phase*, where the lossless supermodes are split by $2\beta_r$. The regime defined by $\Gamma > g_1$ denotes the *broken $\mathcal{PT}$-phase* where the two supermodes have the same frequency, while one of them is dissipating and the other is amplifying.

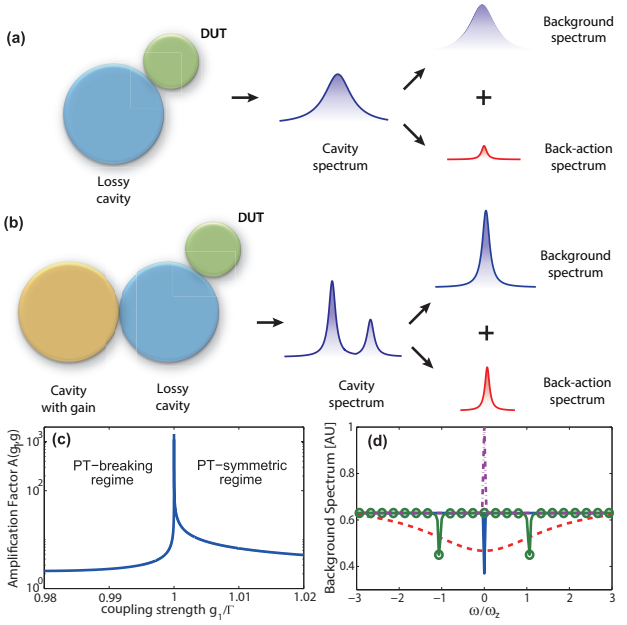

FIG. 1: (Color online) (a) Schematic diagram of a single passive-cavity transducer. (b) $\mathcal{PT}$-cavity-assisted transducer. (c) Amplification factor $A(g_1, g)$ of the back-action spectrum versus the normalized coupling strength g_1/Γ. $A(g_1, g)$ increases very sharply, reaching values as high as 1000, near $g_1 = \Gamma$. (d) Normalized background spectra $S_a(\omega)$ of a passive cavity (red dashed curve), an active cavity (purple dotted curve), and the $\mathcal{PT}$-symmetric cavities in the broken-$\mathcal{PT}$ regime (blue curve) as well as the $\mathcal{PT}$-symmetric regime (green curve with circular symbals). DUT: Device under test.

Rewriting the Hamiltonian (1) in the supermode picture, we find the effective coupling strength between the supermodes and the DUT as [39]

$$g_{\rm eff} = \frac{g\left(\Gamma + \sqrt{\Gamma^2 - g_1^2}\right)}{2\sqrt{\Gamma^2 - g_1^2}}. \tag{2}$$

Clearly, near the transition point $g_1 = \Gamma$, the effective coupling strength $g_{\rm eff}$ is significantly larger than g, implying a drastic enhancement in sensitivity. One can intuitively explain the sensitivity enhancement as follows. The active cavity of the $\mathcal{PT}$ system amplifies the back-action spectrum of the DUT. The gain-loss balance in the $\mathcal{PT}$-symmetric system, on the other hand, makes the background spectrum narrower. The combined effect of these two increases the measurement sensitivity.

In the regime of weak coupling between the cavity and the DUT, we can omit the back-action of the cavity on the DUT. Then the normalized spectrum can be written as [39]

$$S(\omega) \approx G(\omega)\left[S_a(\omega) + A(g_1, g)S_z(\omega)\right]. \tag{3}$$

Here $S_a(\omega)$ is the single-cavity background spectrum calculated by setting $g_1 = 0$; $S_z(\omega) = \mathcal{F}\left[f(t)\mathcal{F}^{-1}S_{zo}(\omega)\right]$

is the back-action spectrum from the DUT, with $S_{zo}(\omega)$ representing the spectrum of the DUT; while $\mathcal{F}$ and $\mathcal{F}^{-1}$ are the Fourier and inverse-Fourier transforms, respectively. The time-domain function $f(t)$ is a form-factor that broadens the back-action spectrum [39]. Equation (3) implies that the interaction between the lossy cavity and the DUT in the $\mathcal{PT}$-system leads to an amplification factor $A(g_1, g)$ acting on the back-action spectrum $S_z(\omega)$ [Fig. 1(c)]. In the $\mathcal{PT}$-breaking regime, as g_1 increases, $A(g_1, g)$ first increases slowly from a very small value and, near the $\mathcal{PT}$ phase transition point, $A(g_1, g)$ increases very sharply, reaching a very high value. When g_1 is further increased and the system enters the $\mathcal{PT}$-symmetric regime, the amplification factor $A(g_1, g)$ drops sharply, to a small value, and continues decreasing with a very slow rate as g_1 is increased.

In Fig. 1(d) we show the background spectrum $S_a(\omega)$ for a lossy cavity and a $\mathcal{PT}$ structure in the $\mathcal{PT}$-symmetric and the broken-$\mathcal{PT}$-symmetric regimes. Due to the presence of gain, the susceptibility coefficient $G(\omega)$ reshapes $S_a(\omega)$, leading to a background spectrum which is significantly narrower than that of a single lossy-cavity. In the $\mathcal{PT}$-symmetric regime, the background spectrum is split into two due to the strong coupling between the cavities, and the split resonances have linewidths narrower than the resonance-linewidth of the single lossy-cavity. Combining the narrower background spectrum $S_a(\omega)$ of a $\mathcal{PT}$ structure with the high amplification factor near the $\mathcal{PT}$-phase transition point leads to a significantly enhanced sensitivity for the CAM.

Optomechanical transducer by $\mathcal{PT}$ breaking.— Hereafter, we will discuss an optomechanical transducer operated near the $\mathcal{PT}$-phase transition point. We first consider that the lossy cavity of the $\mathcal{PT}$ structure supports a mechanical mode. The Hamiltonian of this $\mathcal{PT}$ optomechanical system is obtained from Eq. (1) by replacing the operator z by $(b + b^\dagger)$, where b is the annihilation operator of the mechanical mode. We have obtained the output spectrum [39] of this $\mathcal{PT}$ optomechanical system in a form similar to Eq. (3), and compared it with the single-cavity case in Fig. 2(b).

Next, let us consider a particular $\mathcal{PT}$-symmetric optomechanical transducer realized by two coupled resonators used to detect tiny motions of a mechanical oscillator, e.g., a nanomechanical beam or cantilever, via the optical evanescent field of the passive resonator [Fig. 2(a)] [49]. In order to show the differences between $\mathcal{PT}$ and a single-lossy-cavity optomechanics, we carried out numerical simulations using experimentally accessible values of system parameters: $\Delta = 0$, $\omega_m = 6$ MHz, $\kappa = 20$ MHz, $\gamma_m = 0.2$ MHz, $\gamma = 16$ MHz, $g_1 = 19.8$ MHz, $g = 5$ MHz, where ω_m and γ_m are the frequency and the decay rate of the mechanical oscillator. Since we have deliberately chosen the optomechanical coupling strength g to be very small, the susceptibility coefficient of the single-cavity optomechanical system is very small;

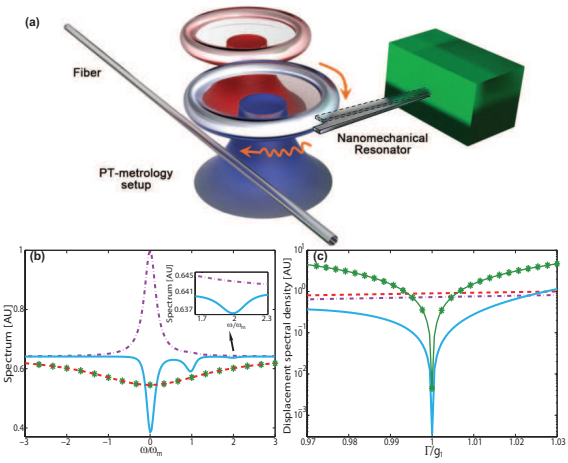

FIG. 2: (Color online) (a) $\mathcal{PT}$-symmetric optomechanical transducer realized by two coupled microresonators, e.g., a silica microtoroid (blue; passive) and a Er^{3+}-doped silica microtoroid (red; active). The passive resonator is coupled to a mechanical oscillator via the optical evanescent field. (b) The normalized output spectra of optomechanical transducers for $\omega_m/\kappa = 0.3$: single-cavity (red dashed curve), single-cavity with gain (purple dot dashed curve), $\mathcal{PT}$-system near the $\mathcal{PT}$-transition point (blue curve), and two-lossy-cavity system near an exceptional point (green curve with star marks). (c) The normalized displacement spectral densities $S_{\mathrm{xx,single}}(\omega_m)$, $S_{\mathrm{xx,gain}}(\omega_m)$, $S_{\mathrm{xx,PT}}(\omega_m)$, and $S_{\mathrm{xx,EP}}(\omega_m)$ of the single passive cavity-optomechanical transducer (red curve), the single active cavity-optomechanical transducer (purple dotted curve), the $\mathcal{PT}$-optomechanical transducer (blue curve), and the two-lossy-cavity transducer (green curve with star symbols) when $\omega_m/\kappa = 0.3$. The measurement sensitivity is enhanced for at least two orders of magnitude by the $\mathcal{PT}$ optomechanical transducer near the transition point, i.e., $S_{\mathrm{xx,PT}}(\omega_m)/S_{\mathrm{xx,single}}(\omega_m) < 10^{-2}$.

thus the back-action spectrum of the mechanical oscillator is masked by the background spectrum of the cavity [red dashed curve in Fig. 2(b)]. The output spectrum of the $\mathcal{PT}$-symmetric transducer [blue curve in Fig. 2(b)] shows two distinct features originating from the gain-loss balance and the one of the amplification mechanism. First, the background spectrum is narrower and the resonance dip located at $\omega/\omega_m = 0$ is amplified. Second, the back-action spectrum of the mechanical motion is clearly seen as a sideband-dip sitting on the background spectrum at $\omega/\omega_m = 1$. We also see the second-order mechanical sideband as a smaller dip located $2\omega_m$ away from the main dip. These confirm that the $\mathcal{PT}$-symmetric structure operated near the $\mathcal{PT}$-phase transition point can detect very weak mechanical motions.

To show the enhancement of the measurement-sensitivity by the $\mathcal{PT}$-symmetric structure, we compare the displacement spectral densities $S_{\mathrm{xx,PT}}(\omega)$ and $S_{\mathrm{xx,single}}(\omega)$ of the $\mathcal{PT}$-symmetric transducer and the single-lossy-cavity transducer. The displacement spec-

tral density $S_{\mathrm{xx,PT}}(\omega)$ and the backaction force spectral density $S_{\mathrm{FF,PT}}(\omega)$ of the $\mathcal{PT}$ optomechanical transducer are found as [11, 39]:

$$S_{\mathrm{xx,PT}}(\omega) = \frac{\Gamma_-^2\,\hbar\Omega_-}{64 g_{\mathrm{eff}}^2 P_{\mathrm{in}}}\left(1+\frac{4\omega}{\Gamma_-^2}\right), \tag{4}$$

$$S_{\mathrm{FF,PT}}(\omega) = \frac{16\hbar g_{\mathrm{eff}}^2 P_{\mathrm{in}}}{\Gamma_-^2\,\Omega_-}\left(1+\frac{4\omega}{\Gamma_-^2}\right)^{-1}, \tag{5}$$

where P_{in} is the input power. It can be shown that $S_{\mathrm{xx,PT}}(\omega)$ and $S_{\mathrm{FF,PT}}(\omega)$ satisfy the Heisenberg inequality [50]: $\sqrt{S_{\mathrm{xx,PT}}(\omega)S_{\mathrm{FF,PT}}(\omega)} \geq \hbar/2$, which implies the possibility of a smaller displacement spectral density if the backaction force spectral density is increased. As shown in Eq. (4), the displacement spectral density $S_{\mathrm{xx,PT}}(\omega)$ is proportional to the decay rate Γ_- of the supermode and inversely proportional to the square of the effective optomechanical coupling strength g_{eff}. Since g_{eff} can be significantly increased near the $\mathcal{PT}$-transition point [Eq. (2)] and Γ_- is very small due to gain-loss balance, the $S_{\mathrm{xx,PT}}(\omega)$ of the $\mathcal{PT}$ optomechanical transducer beats the limits given for the single-cavity case (Fig. 2). The $S_{\mathrm{xx,PT}}(\omega)$ of the $\mathcal{PT}$-symmetric system can be more than two-orders of magnitude smaller than the displacement spectral density $S_{\mathrm{xx,single}}(\omega)$ of the single cavity.

Finally, to show the effect of the gain in the structure, we compare the sensitivity of a system formed by two coupled lossy cavities having loss rates of κ_1 and $\kappa \geq \kappa_1$ with that of the $\mathcal{PT}$-symmetric system formed by coupling a lossy cavity of loss rate κ with a gain cavity of gain rate γ [39]. Note that the loss rates of the cavities coupled to the mechanical mode are the same (i.e., κ) for both systems. For the system of two lossy cavities, there also exists a degenerate point where the eigenfrequencies and the corresponding eigenstates of the system coalesce. This point is generally known as the exceptional point (EP) and has been studied in detail within the field of non-Hermitian Hamiltonians [51]. For such a system the EP takes place at $g_1 = (\kappa-\kappa_1)/2$. Near an EP, we have $g_{\mathrm{eff}} \gg g$, as can be deduced from Eq. (2). For $g_1 > (\kappa-\kappa_1)/2$, the supermodes are split by $2\sqrt{g_1^2-(\kappa-\kappa_1)^2/4}$ but have the same damping rates $(\kappa+\kappa_1)/2$, whereas for $g_1 < (\kappa-\kappa_1)/2$, the supermodes are degenerate at the frequency Δ but have different damping rates $(\kappa+\kappa_1)/2 \mp \sqrt{(\kappa-\kappa_1)^2/4-g_1^2}$. We find the ratio of the amplification factor of the $\mathcal{PT}$-system to that of the two-lossy-cavity system to be $4\gamma^2(\kappa+\kappa_1)/(\kappa-\gamma)^3$, which approaches infinity as the gain-to-loss ratio in the $\mathcal{PT}$-system approaches one. In Fig. 2(b), we see that the normalized spectrum for the two-lossy-cavity (curve with green stars) [39] is similar to that of the single-cavity system when the damping rates of the cavities are the same, and thus the back-action spectrum of the mechanical motion cannot be detected by the two-lossy-cavity system. We observe a similar decrease of the displacement spectral density for $\mathcal{PT}$ and EP systems near the transition point, but the $\mathcal{PT}$-system performs much better because the effective damping rate of the $\mathcal{PT}$-system is much smaller due to the gain-loss balance (Fig. 2(c)).

The enhancement of sensitivity in the EP (i.e., lossy system; no optical gain) and $\mathcal{PT}$-symmetric (i.e., with optical gain balancing the loss) systems stems from the square-root-topology [52, 53] of complex energy surfaces in their parameter space. This leads to significant changes in their output spectra even for infinitesimally small perturbations. This also provides a significant enhancement in the optomechanical coupling and the back-action spectrum, with the effective coupling reaching its maximum exactly at the EP (or $\mathcal{PT}$-transition point). In order to detect and resolve very small changes in the spectrum of a system, the linewidths of the resonances should be sufficiently narrow. Since the linewidths of the resonances in a $\mathcal{PT}$-symmetric system are narrower than those in an EP system, because of the gain-loss balance in the former, $\mathcal{PT}$-symmetric systems are superior to EP systems for sensing purposes; although both have the same square-root topology in their respective parameter spaces. For a single passive cavity mode, single active cavity mode, or a single microlaser mode, which is described by an isolated single first-order pole, such a square-root topology is not present and the lineshapes are symmetric and Lorentzian. Thus, such systems cannot enhance the optomechanical coupling strength, and they cannot modify the back-action spectrum. However, an active cavity or a microlaser can modify the background spectrum, making it much narrower than that for a passive cavity. Therefore, a perturbation that cannot be observed or resolved in the spectrum (due to the large background spectrum of a passive cavity) can be resolved by an active cavity having sufficient optical gain (i.e., a linewidth narrower than that of the passive cavity) or by a microlaser due to their narrower background spectrum.

We should note that enhanced-sensing at the EPs has been previously discussed, for single-nanoparticle detection, by J. Wiersig [54] who showed that the sensitivity of single-nanoparticle detection using the mode-splitting method [17] in a single whispering-gallery-mode passive cavity can be improved by three-fold if the microcavity is first brought to an EP by two localized perturbations [51, 55] before the arrival of the nanoparticle. It was also suggested that a single active microcavity with optical gain could be used to better resolve the splitting due to reduced linewidth [54] similar to what was reported in Refs. [18, 56] . Our work goes beyond Ref. [54], bringing together optomechanics and the concepts of EP and $\mathcal{PT}$-symmetry in coupled microcavities to build an optomechanical transducer for enhanced metrology for displacement measurement of nanobeams and cantilevers.

Conclusion.— We have proposed $\mathcal{PT}$-metrology as an efficient approach to improve the sensitivity and detec-

tion limit of CAM beyond what is attainable in conventional settings, where the system to be measured is coupled to a lossy cavity. In $\mathcal{PT}$-metrology, a second cavity with gain is coupled to the lossy cavity to compensate its loss, thereby increasing the quality factor of the effective optical mode used to detect the weak signal, and enhancing the effective cavity-DUT coupling strength. The enhancement is remarkable, especially near the transition point, where the supermodes of the system coalesce in their frequencies, and can be further enhanced as the gain-to-loss ratio approaches unity. We have showed that it is possible to realize an ultra-sensitive optomechanical transducer whose *sensitivity is at least two orders of magnitude* better than single-cavity optomechanical transducers. Our approach can be used for improving the performance of nanoparticle sensors [54], navigation systems, gravity-wave detectors and other cavity-assisted detection schemes. Finally, the asymmetric lineshapes near an EP have recently shown to be described as genuine Fano resonances [57–59], suggesting a similarity of the underlying physics for sensitivity enhancement in Fano- and EP-based sensors. This issue requires further studies as it is still unclear whether all resonances that can be fit by the Fano formula have their origin in an EP.

YXL and JZ are supported by the National Basic Research Program of China (973 Program) under Grant No. 2014CB921401, the Tsinghua University Initiative Scientific Research Program, and the Tsinghua National Laboratory for Information Science and Technology (TNList) Cross-discipline Foundation. JZ is supported by the NSFC under Grant Nos. 61174084, 61134008, 60904034. YXL is supported by the NSFC under Grant Nos. 10975080, 61025022, 91321208. F.N. is partially supported by the RIKEN iTHES Project, MURI Center for Dynamic Magneto-Optics via the AFOSR award number FA9550-14-1-0040, and a Grant-in-Aid for Scientific Research (A). LY and SKO are supported by the ARO Grants No. W911NF-12-1-0026 and W911NF-16-1-0339.

* Electronic address: jing-zhang@mail.tsinghua.edu.cn
† Electronic address: ozdemir@wustl.edu

[1] R. Schnabel, N. Mavalvala, D. E. McClelland, and P. K. Lam, Quantum metrology for gravitational wave astronomy, Nat. Comm. **1**, 121 (2010).
[2] N. Zhao, J. L. Hu, S. W. Ho, J. T. K. Wan, and R. B. Liu, Atomic-scale magnetometry of distant nuclear spin clusters via nitrogen-vacancy spin in diamond, Nat. Nanotechnology **6**, 242 (2011).
[3] F. Z. Shi, X. Kong, P. F. Wang, F. Kong, N. Zhao, R. B. Liu, and J. F. Du, Sensing and atomic-scale structure analysis of single nuclear-spin clusters in diamond, Nat. Physics **10**, 21 (2014).
[4] E. Sánchez-Burillo, J. Duch, J. Gómez-Gardeñes, and D. Zueco, Quantum navigation and ranking in complex networks, Sci. Rep. **2**, 605 (2012).
[5] P. Marks, Quantum positioning system steps in when GPS fails, New Scientist **222**, 19 (2014).
[6] H. M. Wiseman, Adaptive phase measurements of optical modes: Going beyond the marginal Q distribution, Phys. Rev. Lett. **75**, 4587-4590 (1995).
[7] G. Y. Xiang, B. L. Higgins, D. W. Berry, H. M. Wiseman, and G. J. Pryde, Entanglement-enhanced measurement of a completely unknown optical phase, Nat. Photon. **5**, 43-47(2011).
[8] A. A. Clerk, M. H. Devoret, S. M. Girvin, F. Marquardt, and R. J. Schoelkopf, Introduction to quantum noise, measurement, and amplification, Rev. Mod. Phys. **82**, 1155 (2010).
[9] I. Siddiqi, R. Vijay, M. Metcalfe, E. Boaknin, L. Frunzio, R. J. Schoelkopf, and M. H. Devoret, Dispersive measurements of superconducting qubit coherence with a fast latching readout, Phys. Rev. B **73**, 054510 (2006).
[10] M. Aspelmeyer, T. J. Kippenberg, and F. Marquardt, Cavity optomechanics, Rev. Mod. Phys. **86**, 1391 (2014).
[11] J. M. Dobrindt and T. J. Kippenberg, Theoretical analysis of mechanical displacement measurement using a multiple cavity mode transducer, Phys. Rev. Lett. **104**, 033901 (2010).
[12] C. Guerlin, J. Bernu, S. Deléglise, C. Sayrin, S. Gleyzes, S. Kuhr, M. Brune, J.-M. Raimond, and S. Haroche, Progressive field-state collapse and quantum non-demolition photon counting, Nature **448**, 889 (2007).
[13] A. Szorkovszky, A. A. Clerk, A. C. Doherty, and W. P. Bowen, Mechanical entanglement via detuned parametric amplification, New J. Phys. **16**, 043023 (2014).
[14] C. Galland, N. Sangouard, N. Piro, N. Gisin, and T. J. Kippenberg, Heralded single-phonon preparation, storage, and readout in cavity optomechanics, Phys. Rev. Lett. **112**, 143602 (2014).
[15] A. Nunnenkamp, K. Børkje, and S. M. Girvin, Single-photon optomechanics, Phys. Rev. Lett. **107**, 063602 (2011).
[16] P. Rabl, Photon blockade effect in optomechanical systems, Phys. Rev. Lett. **107**, 063601 (2011).
[17] J. Zhu, Ş. K. Özdemir, Y. Xiao, L. Li, L. He, D. Chen, and L. Yang , On-chip single nanoparticle detection and sizing by mode splitting in an ultrahigh-Q microresonator, Nature Photonics **4**, 46-49 (2010).
[18] L. He, Ş. K. Özdemir, J. Zhu, W. Kim, and L. Yang, Detecting single viruses and nanoparticles using whispering gallery microlasers, Nat. Nanotechnology **6**, 428-432 (2011).
[19] C. M. Bender, Making sense of non-Hermitian Hamiltonians, Rep. Prog. Phys. **70**, 947-1018 (2007).
[20] A. A. Sukhorukov, Z. Xu, and Y. S. Kivshar, Nonlinear suppression of time reversals in $\mathcal{PT}$-symmetric optical couplers, Phys. Rev. A **82**, 043818 (2010).
[21] H. Ramezani, T. Kottos, R. El-Ganainy, and D. N. Christodoulides, Unidirectional nonlinear $\mathcal{PT}$-symmetric optical structures, Phys. Rev. A **82**, 043803 (2010).
[22] Z. Lin, H. Ramezani, T. Eichelkraut, T. Kottos, H. Cao, and D. N. Christodoulides, Unidirectional invisibility induced by $\mathcal{PT}$-symmetric periodic structures, Phys. Rev. Lett. **106**, 213901 (2011).
[23] X. Zhu, L. Feng, P. Zhang, X. Yin, and X. Zhang, One-way invisible cloak using parity-time symmetric transformation optics, Opt. Lett. **38**, 2821 (2013).

[24] C. Hang, G. Huang, and V. V. Konotop, $\mathcal{PT}$ symmetry with a system of three-level atoms, Phys. Rev. Lett. **110**, 083604 (2013).

[25] G. S. Agarwal and K. Qu, Spontaneous generation of photons in transmission of quantum fields in $\mathcal{PT}$-symmetric optical systems, Phys. Rev. A **85**, 031802 (2012).

[26] H. Benisty, A. Degiron, A. Lupu, A. D. Lustrac, S. Chénais, S. Forget, M. Besbes, G. Barbillon, A. Bruyant, S. Blaize, G. Lérondel, Implementation of $\mathcal{PT}$ symmetric devices using plasmonics: principle and applications, Opt. Exp. **19**, 18004 (2011).

[27] N. Lazarides and G. P. Tsironis, Gain-driven discrete breathersin $\mathcal{PT}$-symmetric nonlinear metamaterials, Phys. Rev. Lett. **110**, 053901 (2013).

[28] Y. Lumer, Y. Plotnik, M. C. Rechtsman, and M. Segev, Nonlinearly induced $\mathcal{PT}$ transition in photonic systems, Phys. Rev. Lett. **111**, 243905 (2013).

[29] H. Jing, Ş. K. Özdemir, X.-Y. Lü, J. Zhang, L. Yang, and F. Nori, $\mathcal{PT}$-Symmetric Phonon Laser Phys. Rev. Lett. **113**, 053604 (2014).

[30] A. Guo, G. J. Salamo, D. Duchesne, R. Morandotti, M. Volatier-Ravat, V. Aimez, G. A. Siviloglou, and D. N. Christodoulides, Observation of $\mathcal{PT}$-symmetry breaking in complex optical potentials, Phys. Rev. Lett. **103**, 093902 (2009).

[31] C. E. Rüter, K. G. Makris, R. El-Ganainy, D. N. Christodoulides, M. Segev and D. Kip, Observation of parity-time symmetry in optics, Nat. Phys. **6**, 192 (2010).

[32] A. Regensburger, C. Bersch, M. Miri, G. Onishchukov, D. N. Christodoulides, and U. Peschel, Parity-time synthetic photonic lattices, Nature **488**, 167 (2012).

[33] L. Feng, Y. Xu, W. S. Fegadolli, M. Lu, J. E. B. Oliveira, V. R. Almeida, Y. Chen, and A. Scherer, Experimental demonstration of a unidirectional reflectionless parity-time metamaterial at optical frequencies, Nat. Mater. **12**, 108 (2012).

[34] J. Schindler, A. Li, M. C. Zheng, F. M. Ellis, and T. Kottos, Experimental study of active LRC circuits with $\mathcal{PT}$ symmetries, Phys. Rev. A **84**, 040101(R) (2011).

[35] S. Bittner, B. Dietz, U. Gnther, H. L. Harney, M. Miski-Oglu, A. Richter, and F. Schäfer, $\mathcal{PT}$ symmetry and spontaneous symmetry breaking in a microwave billiard, Phys. Rev. Lett. **108**, 024101 (2012).

[36] C. M. Bender, B. K. Berntson, D. Parker, E. Samuel, Observation of $\mathcal{PT}$ phase transition in a simple mechanical system Am. J. Phys. **81**, 173-179 (2013).

[37] N. Bender, S. Factor, J. D. Bodyfelt, H. Ramezani, D. N. Christodoulides, F. M. Ellis, and T. Kottos, Observation of asymmetric transport instructures with active nonlinearities, Phys. Rev. Lett. **110**, 234101 (2013).

[38] B. Peng, Ş. K. Özdemir, F. C. Lei , F. Monifi, M. Gianfreda, G. L. Long, S. H. Fan, F. Nori, C. M. Bender, and L. Yang , Parity-time-symmetric whispering-gallery microcavities, Nat. Phys. **10**, 394-398 (2014).

[39] See Supplementary Materials for more details, which includes Refs. [40-48].

[40] C. M. Bender, D. C. Brody, and H. F. Jones, Complex extension of quantum mechanics, Phys. Rev. Lett. **89**, 270401 (2002).

[41] C. M. Bender, D. C. Brody, H. F. Jones, and B. K. Meister, Faster than Hermitian quantum mechanics, Phys. Rev. Lett. **98**, 040403 (2007).

[42] J. Stein, in *Digital Signal Processing: A Computer Science Perspective*, edited by J. G. Proakis (Wiley, 2000), p. 115.

[43] B. Peng, Ş. K. Özdemir, W. Chen, F. Nori and L. Yang, What is and what is not electromagnetically induced transparency in whispering-gallery microcavities, Nat. Comm. **5**, 5082 (2014).

[44] Y. Zhang, Y. Zhen, O. Neumann, J. K. Day, P. Nordlander, N. J. Halas, Coherent anti-Stokes Raman scattering with single-molecule sensitivity using a plasmonic Fano resonance, Nat. Comm. **5**, 4424 (2014).

[45] A. K. Dmitry, P. Zhenying, I. K. Arseniy and A. K. Leonid, Quantum spectroscopy of plasmonic nanostructures, Phy. Rev. X **4**, 011049 (2014).

[46] A. Schawlow, and C. Townes, Infrared and optical masers. Phys. Rev. **112**, 1940-1949 (1958).

[47] J.-Q. Liao, H. K. Cheung, and C. K. Law, Spectrum of single-photon emission and scattering in cavity optomechanics, Phys. Rev. A **85**, 025803 (2012).

[48] X.-W. Xu, Y. J. Li, and Y. X. Liu, Photon-induced tunneling in optomechanical systems, Phys. Rev. A **87**, 025803 (2013).

[49] G. Anetsberger, O. Arcizet, Q. P. Unterreithmeier, R. Riviere, A. Schliesser, E. M. Weig, J. P. Kotthaus and T. J. Kippenberg, Near-field cavity optomechanics with nanomechanical osillators, Nat. Phys. **5**, 909-914 (2009)

[50] V. B. Braginsky and F. Khalili, Quantum measurement (Cambridge University Press, Cambridge, England, 1992).

[51] B. Peng, Ş. K. Özdemir, S. Rotter, H. Yilmaz, M. Liertzer, F. Monifi, C. M. Bender, F. Nori, and L. Yang, Loss-induced suppression and revival of lasing, Science **346**, 328 (2014).

[52] W. D. Heiss, The physics of exceptional points, J. Phys. A: Math. Theor. **45**, 444016 (2012).

[53] E. Hernández, A. Jáuregui, and A. Mondragón, Non-Hermitian degeneracy of two unbound states, J. Phys. A: Math. Gen. **39**,10087 (2006).

[54] J. Wiersig, Enhancing the sensitivity of frequency and energy splitting detection by using exceptional points: application to microcavity sensors for single-particle detection, Phys. Rev. Lett. **112**, 203901 (2014).

[55] J. Zhu, Ş. K. Özdemir, L. He, L. Yang, Opt. Express **18**, 23535 (2010).

[56] L. He, Ş. K. Özdemir, J. Zhu, and L. Yang, Ultrasensitive detection of mode splitting in active optical microcavities, Phys. Rev. A **82**, 053810 (2010).

[57] L. Schwarz, H. Cartarius, G. Wunner, W. D. Heiss and J. Main, Fano resonances in scattering: an alternative perspective, Eur. Phys. J. D **69**, 196 (2015).

[58] W. D. Heiss, G. Wunner, Fano-Feshbach resonances in two-channel scattering around exceptional points, Eur. Phys. J. D **68**, 284 (2014).

[59] A. I. Magunov, I. Rotter, and S. I. Strakhova, Fano resonances in the overlapping regime, Phys. Rev. B **68**, 245305 (2003).